Journal of Materials Chemistry B

Accepted Manuscript

ROYAL SOCIETY OF CHEMISTRY

www.rsc.org/materialsB

Journal Name

RSCPublishing

ARTICLE

Synergistic effects of a novel free-standing reduced graphene oxide film and surface coating fibronectin on morphology, adhesion and proliferation of mesenchymal stem cells

Cite this: DOI: 10.1039/x0xx00000x

Received 00th January 2012,
Accepted 00th January 2012

DOI: 10.1039/x0xx00000x

www.rsc.org/

Lin Jin, [a,b] Zhiping Zeng, [c] Shreyas Kuddannaya,[a] Dan Yue,[b] Jingnan Bao,[a] Zhenling Wang*[b], Yilei Zhang, *[a]

Graphene films have broad applications in engineering, energy and biomedical applications. The cost-effective, eco-friendly and easy to scale-up fabrication methods of graphene films are always highly desired. In this work, we develop a novel fabrication method of free-standing reduced graphene oxide (RGO) films by vacuum filtration of graphene oxide aqueous solution through a nanofiber membrane combining with chemical reduction. Instead of smooth surface, the generated RGO films have nanoscale patterns transferred from the nanofiber membrane and controlled in a large range by varying parameters of electrospinning process. The cellular culture results of the human marrow mesenchymal stem cells (hMSCs) show that the fibronectin modified RGO films could exhibit excellent biocompatibility, which could be attributed to the synergistic effects of the RGO films including both the surface morphology and the fibronectin modification. The novel fabrication method greatly enhances the fabrication capability and the potential applications of graphene films for cell culture, tissue engineering as well as other engineering and biomedical applications.

1. Introduction

Graphene, a two-dimensional monolayer of sp^2-bonded carbon atoms, has attracted more and more research interests in various scientific and technological fields[1-12] due to its excellent electrical and mechanical properties as well as extraordinary large surface area (~2600m^2 per gram). With those properties, graphene has been successfully applied in a variety of engineering and biological applications, including disease diagnosis,[13,14] sensitive biosensing,[15] targeting and photothermal therapy,[16] cellular imaging,[17] drug delivery and tissue engineering.[17-21] Recently, free-standing paper-like or foil like graphene films have been fabricated due to their intriguing electronic, optical and mechanical properties, which have broad applications in the technological society, including tissue engineering, electrical batteries, supercapacitors, etc.[12, 22-26]

Significant progress has been made in fabrication of the free-standing graphene films, for example, porous anodized aluminium oxide (AAO) filter discs have been used in a vacuum filtration method to produce the graphene oxide paper.[1,22] Free-standing graphite oxide membrane has also been fabricated using self-assembled method.[6] However, the broad applications of the free-standing graphene films are still limited by the fabrication process due to the high cost, the low productivity, and the difficulty to fabricate large size films. Furthermore, surface morphology of the free-standing graphene films are very important for many applications, such as the cell culture or tissue engineering, where the cell-substrate interactions are significantly affected by the substrate morphology.[23-25] For current fabrication processes, the generated surface morphology of the free-standing graphene films depends on the fabrication process and is lack of control.

In this study, we developed a novel fabrication method to produce free-standing reduced graphene oxide (RGO) films with controllable nanofiber patterns by vacuum filtration of graphene oxide aqueous solution through a nanofiber membrane combining with chemical reduction. Instead of the AAO filter, the nanofiber membrane was used and prepared using the electrospinning method, which is a well-developed process with features such as low cost, high productivity, and easy to fabricate large size membranes.[7, 26] Furthermore, the diameter and porosity of the nanofiber membrane could be controlled in a large range[7] comparing with the AAO filter, which enables a large range, controllable nanofiber patterns generated on the free-standing graphene films. We selected human mesenchymal stem cells (hMSCs) as the model cell to investigate the biocompability of the obtained RGO films before and after fibronectin (FN) functionalization comparing with TCPs, which demonstrated that the RGO films could offer an excellent micro-environment for cell adhesion and proliferation. Together with the outstanding mechanical properties of the RGO films, the modified substrates are promising candidates in engineering and biological applications, such as electroactive substrates/scaffolds, drug delivery and biosensors.

2. Experimental Section

2.1 Preparation of GO

Graphene oxide (GO) was synthesized from natural graphite using a modified Hummers method.[27, 28] DI water was used in all experiments. GO suspension was achieved by ultrasonication of the GO solution (1mg/mL) using an ultrasonic cleaner (KQ-100, frequency 40 kHz, output power 100W). The obtained brown dispersion was then subjected to centrifugation at 3,000 r.p.m. for 30 min to remove any unexfoliated graphene oxide (usually nothing present).

2.2 Fabrication of RGO film and FN modified RGO film

Nanofibers were fabricated using electrospinning as described in the previous report.[29] Briefly, 10.0% PVC (Mn=40k) (THF)/N, N-dimethyl-formamide (DMF) (v:v = 8:2) was under constant stirring until the mixture was clear, viscous, and homogenous. The mixture solution was fed into a syringe capped with a 0.22 gauge blunt-tripped needle and driven by a syringe pump (Langer CO., Baoding, China) at a speed of 1.0 mL/h. The distance between the tip of the syringe needle and the collector was 10 cm and a voltage of 12 kV was applied by a high voltage DC power supply (Dongwen High Voltage, Tianjing, China).

A GO film was formed automatically on the filter membrane (PVC nanofibers), which was then peeled off and dried at 80°C for 24 hours. By dipping the formed GO film in an HI aqueous solution (55%) at 100°C for 1 hour, the RGO film was obtained after the chemical reduction, which was then washed repeatedly with ethanol to remove any residual HI.[12] In order to functionalize the RGO film with FN (Sigma-Aldrich Singapore), the films were immersed in a 0.1% poly-L-lysine (PLL) solution for 1 h at room temperature, followed by washing with phosphate buffered saline (PBS) buffer three times. The films were then immersed in a FN solution with 0.1 mg/mL and incubated at 4°C overnight. Prior to cells seeding, the films were rinsed with PBS buffer three times.

2.3 Characterization of GO film and RGO film

The morphology of the GO and RGO films was measured using a Cypher™ atomic force microscope (AFM) in tapping mode and operated under ambient conditions and a scanning electron microscope (SEM, Hitachi S-4800) at an acceleration voltage of 10 kV. The mechanical tensile stress-strain response of those films was evaluated using a micro-tensile testing machine (Sans-GB T528, Shenzhen, China). The chemical composition was examined by Raman spectrum (RIGAKU Co., Japan).

2.4 Isolation and culture of mesenchymal stem cells

hMSCs were obtained by side population of human PLC/PRF/5 cell line (ATCC, Manassas, VA, USA) with flow cytometry based on Hoechst 33342 (Invitrogen, Carlsbad, CA, USA). After flow cytometry sorting, hMSCs were kept in complete DMEM medium for experiments within 2 hours.

The FN modified/unmodified graphene films were cut to fit into 24-well tissue culture plates, then sterilized by soaking in a solution of 70% ethanol and 30% PBS for 12 hours, followed by washing several times with PBS. hMSCs were seeded onto the films and TCPs at a cell density of 1.5×10^4 cell/well with 0.5 mL DMEM supplemented with 10% (v/v) FBS. All the cells were incubated under humidified conditions with 5% CO_2 at 37ºC.

2.5 Fluorescence detection

To assess cell viability, samples were incubated with 5ug/mL Alexa Fluor 546® phalloidin (red, Sigma-Aldrich) and 5ug/mL Hoechst 33258 (blue, Sigma-Aldrich) in culture medium for 20 min at 37°C, then fixed with 3.7% paraformaldehyde for 30 min and imaged under a Leica TCS-SP2 Confocal Microscope (Leica, Germany) using TCS Leica Software 2.61.

2.6 Assessment of cellular morphology

Cellular morphology on the scaffold was visualized using SEM. The cells were fixed with 3% glutaraldehyde for 24 h and dehydrated using increasing ethanol/water concentrations (25%, 50%, 70%, 80%, 90%, 95% and absolute ethanol for 30 min each),[29] and dried in air overnight. Platinum/palladium was coated on the sample with 10 nm in thickness using a sputter coater and imaged with SEM.

2.7 Cell adhesion and proliferation on FN modified RGO films

Cellular adherence and proliferation were quantified at various time points based on a DNA analysis method.[30, 31] Briefly, PicoGreen® DNA quantification (Quant-iT Picogreen, P7589, Invitrogen) was used to measure the DNA content of the samples incubated with hMSCs for cellular adherence and proliferation. After 4 hours, 1, 3, and 7 days incubation, cells were lysed with 1% triton X-100 and subjected to several freeze-thaw cycles. From the lysates (25 µL), DNA content was calculated using PicoGreen® DNA quantification (Quant-iT Picogreen, P7589, Invitrogen) according to manufacturer's instructions. Briefly, 75 µL of Picogreen® reagent was incubated with each lysate protected from light at room temperature for 5 minutes. Fluorescence of the samples was measured at 485/535 nm using a Victor3 multilabel fluorescence plate reader (PerkinElmer, USA). Samples were assayed at 4 hours, 1, 3 and 7 days and the DNA contents were determined with reference to a standard curve. The cell number was converted from the DNA value and plotted.

2.8 Statistical Analysis

Data were expressed as mean ± standard deviation. Statistical analyses were performed with the t-test. All data were analysed with the SPSS software (version 11.0).

3. Results and discussion

3.1 Fabrication and morphology

The fabrication process of the reduced graphene oxide film was shown in Figure 1. Using the electrospinning PVC nanofibers as the filter membrane, the GO aqueous solution (1mg/mL) was filtered using a vacuum filtration process. The obtained GO sheets in the aqueous solution were characterized (Figure S1). A single graphene oxide sheet was clearly shown in the AFM image (Figure S1A). The average thickness of the graphene oxide sheets is around 1.0 nm (Figure S1B), which is slightly larger than the monolayer graphene (0.776 nm) due to the oxygen functional groups on the basal planes and edges of the GO.[1, 7] The original GO nanosheets were of irregular shape with lateral dimensions ranging from several hundred nanometers to several micrometers (Figure S1C). The experimental results indicated that the GO suspension has a good dispersion and size distribution.

After peeling off from the nanofiber membrane and drying, the

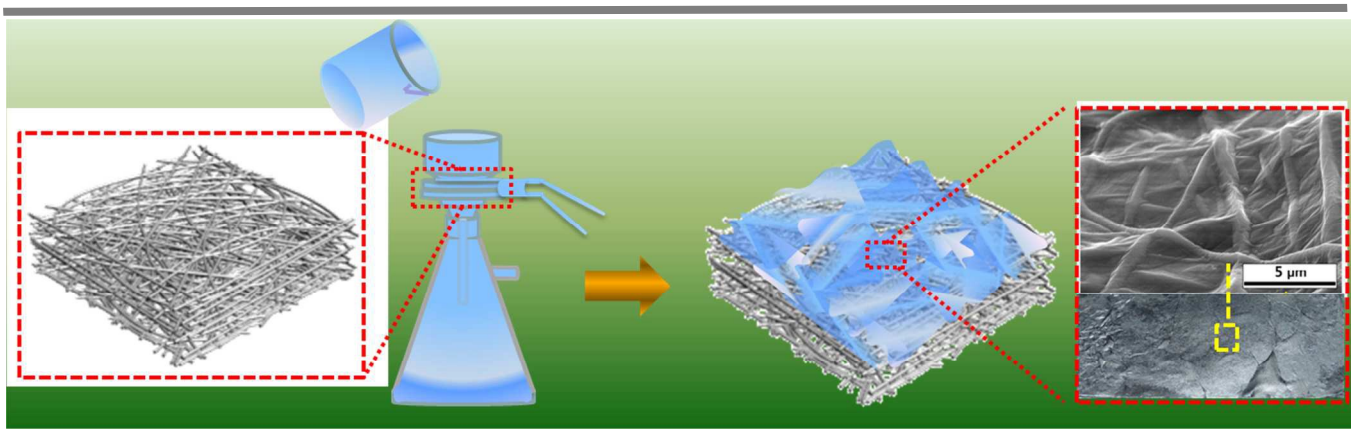

Figure 1. Schematic diagram of the fabrication process of RGO films by electrospinning and vacuum filtration. The electrospun nanofibers were used as the filter membrane for the vacuum filtration to generate GO films before chemical reduction.

GO film exhibits yellow colour (Figure 2A). After chemical reduction, the obtained RGO film becomes dark brown with obvious metallic luster (Figure 2B). The GO film formation process was also observed. During the vacuum filtering, single GO sheet attached on the nanofiber surface (Figure 2C) and eventually formed a GO film on the nanofiber membrane (Figure 2D), which will be peeled off for chemical reduction to obtain the RGO film. Comparing to the traditional filtration membranes, there are two ways to control the p-atterns of the graphene films using the nanofiber membranes. First, nanofibers patterns left on the graphene film can be easily determined by the nanofiber properties, such as nanofiber diameter, density, porosity, pore size of the membrane, etc. (Figure 2E). In this study, the above mentioned nanofiber properties could be well controlled by adjusting the electrospinning process parameters, such as flow rate, applied voltage, electrospun solution, etc.[7] Second, film deformation on the irregular nanofiber membrane will rough film morphology. Generally, with the increase of the RGO film thickness, the nanofiber patterns on the RGO film surface become rougher (Figure 2F).

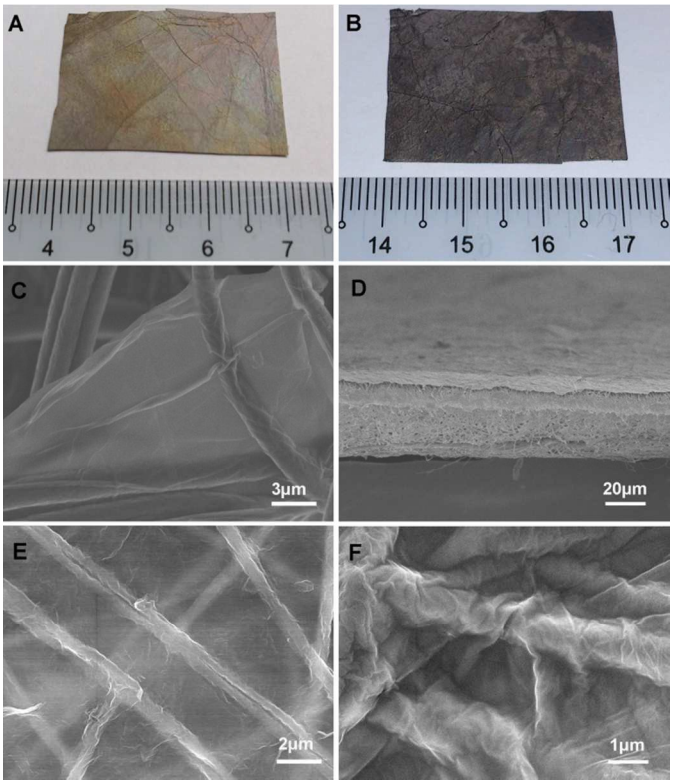

Figure 2. Optical photos of (A) the GO film and (B) the RGO film; SEM images of (C) a single GO sheet attached on the surface of nanofibers, (D) a GO film formed on a nanofiber membrane after vacuum filtering; RGO film after the chemical reduction with nanofiber patterns (E) thin film with relatively smooth surface, and (F) thick film with relatively rough surface.

3.2 Chemical characterization

The Raman, XRD and FTIR spectrum characterization of the GO and RGO films were conducted (Figure 3). The Raman spectrum of the GO film shows GO characteristic peaks (G peaks ~1590 cm^{-1} and D peaks ~1320 cm^{-1}). After HI acid reduction, the G peak of the RGO film is located at 1592 $cm^{-1}$and the D peak increases obviously (Figure 3A). The locations of the two peaks for the RGO film are close to the values of pristine graphite, which indicates the successful reduction of the GO films by HI acid dense treatment.[32-34] In the XRD spectrum of the GO film, a strong reflection with peak at $2\theta = 9.89°$ appeared (Figure 3B), which can be attributed to the (002) reflection.[35] After the chemical reduction, a large shift of (002) reflection peak from 9.9° to 24.12° was observed in the XRD pattern of RGO film, which is most likely due to the elimination of the oxygen containing groups in lower d-spacing.[35-36] The Fourier transform infrared (FTIR) spectrum (Figure 3C) confirmed that the dominant oxygen-containing groups, including -OH and C=O stretching of carboxylic acid and ester groups, had almost been r-emoved completely after the chemical reduction.[35, 36] These results indicated that we have successfully fabricated RGO film by vacuum filtration of graphene oxide aqueous solution through a nanofiber membrane combining with chemical reduction.

3.3 Mechanical property

The tensile measurements demonstrate that the GO and RGO films exhibit typical deformation of graphene films under tensile loading at room temperature (Figure 4). The typical fracture strengths of the GO and RGO films are 8.3±0.3MPa and 13.6±0.5MPa, at ultimate elongations of 6.3±0.2% and 3.8±0.15%, respectively, which are good enough to meet the requirements for many tissue engineering applications. The increase of fracture strength for RGO films could probably be attributed to the increase of the graphene sheets stacking

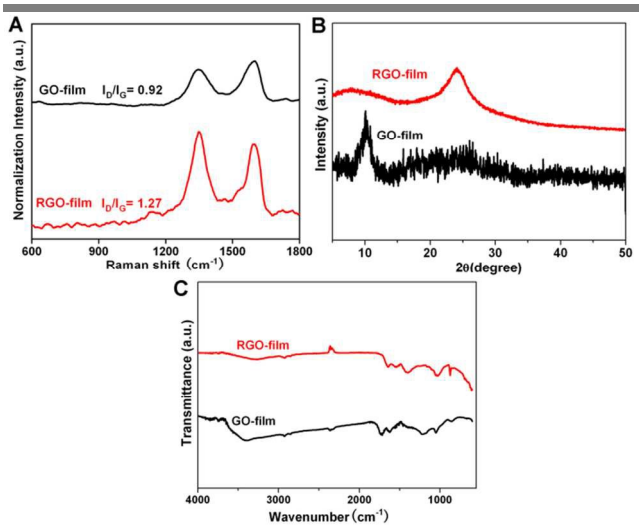

Figure 3. The chemical characterizations of GO film before and after reduction. The spectrum of Raman (A), XRD (B) and FTIR (C).

during the chemical reduction. Comparing with the previous results using the AAO filter[1], the strain and strength values of the obtained GO and RGO films are not as large due to the usage of the nanofiber filter, which has a higher irregularity that may affect the packing of graphene nano-sheets and a trade-off to obtain controllable nanofiber patterns on the free-standing films.

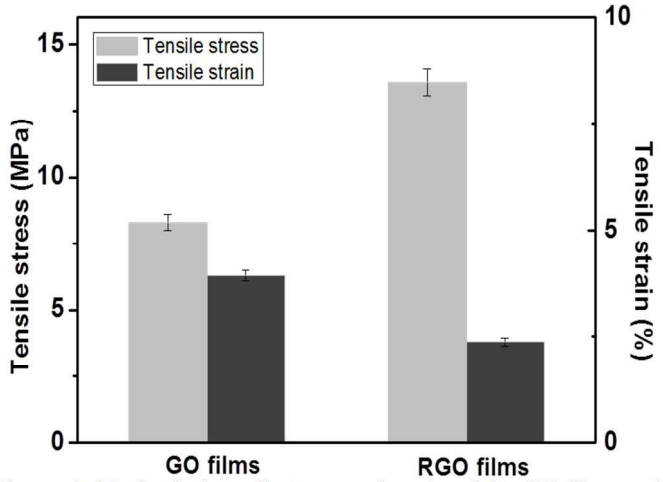

Figure 4. Mechanical tensile stress and strain of the GO films and the RGO films.

3.4 Biocompatible Evaluation

Substrate chemical properties could be modified by surface functionalization to reduce hydrophobicity or increase biocompatibility of the RGO films. The large surface area of graphene films makes them suitable for surface functionalization with different functional groups, such as amine, carboxylic acid and hydroxyl groups, to study and control cellular responses. Previous reports have studied graphene substrates for cell adhesion, proliferation and differentiation.[37-42] A positive effect on cellular responses has been found in the term of mesenchymal stem cells (MSCs) and human osteoblasts cultured on the functional graphene substrates.[37-42] For example, graphene-nanofibers hybrid scaffolds have been demonstrated to promote neural stem cells (NSCs) growth and differentiation into oligodendrocytes,[43] fluorinated graphene effectively induced higher proliferation and stronger polarization of mesenchymal stem cells (MSCs).[40]

For surface functionalization, fibronectin (FN) is a critical extracellular matrix (ECM) protein affecting the cells morphology, migration, proliferation and differentiation. For cell culture, human mesenchymal stem cells (hMSCs) are mononuclear cell population that could be isolated from adult bone marrow. They provide a promising cell source for tissue engineering and regenerative medicine because of their multipotency and ready availability form mesenchymal origins.[44-46] These cells could also serve as a good model for testing properties of culture substrates because they could differentiate into multiple lineages depending on both physical and chemical properties of the substrates.

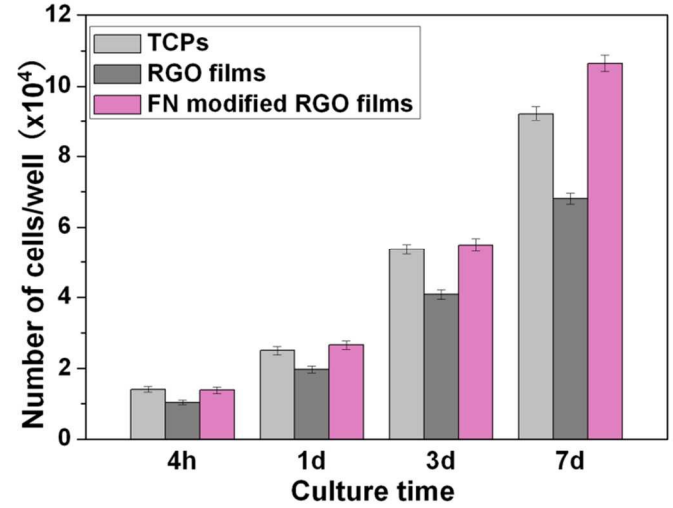

Figure 5. The proliferation of hMSCs cultured on TCPs, RGO and FN modified RGO films for various incubation periods. n=3.

In this study, in order to evaluate the biocompatibility of the modified RGO films, hMSCs were cultured with a cell density of 1.5×10^4/well and after four hours culture, the cellular attachment of hMSCs on the TCPs, the RGO and the FN modified RGO films are 93%, 68.7% and 91.3% respectively, which indicate that FN coated RGO films could significantly enhance cell adhesion (Figure 5). After one day culture, the cellular amount of hMSCs on the TCPs, the RGO and the FN modified RGO films are 2.51×10^4, 1.98×10^4, and 2.66×10^4, respectively. The cell number of the modified RGO films is slightly more compared to that on the TCPs. On day 3, the cell number of the modified RGO films is much higher than that on the unmodified RGO films, which shows that hMSCs on the modified RGO films remained metabolically active and continued to proliferate, and possessed a much higher proliferation activity compared to the unmodified RGO film. After seven days culture, the number of cells on the modified RGO films was increased to 10.65×10^4, comparing with only 6.81×10^4 on the unmodified RGO films, 9.23×10^4 on the TCPs. These results suggest that the FN coated on the RGO films has a significant effect on the cell proliferation, which is consistent with the previous studies.[45,46] Considering the excellent mechanical properties of these obtained films, they are excellent candidates for tissue engineering and biomedical devices, particularly when high mechanical strengths are required.

F-actin of the hMSCs was visualized using Alexa Fluor 546® phalloidin, and cell nuclei were stained with Hoechst 33258. TCPs

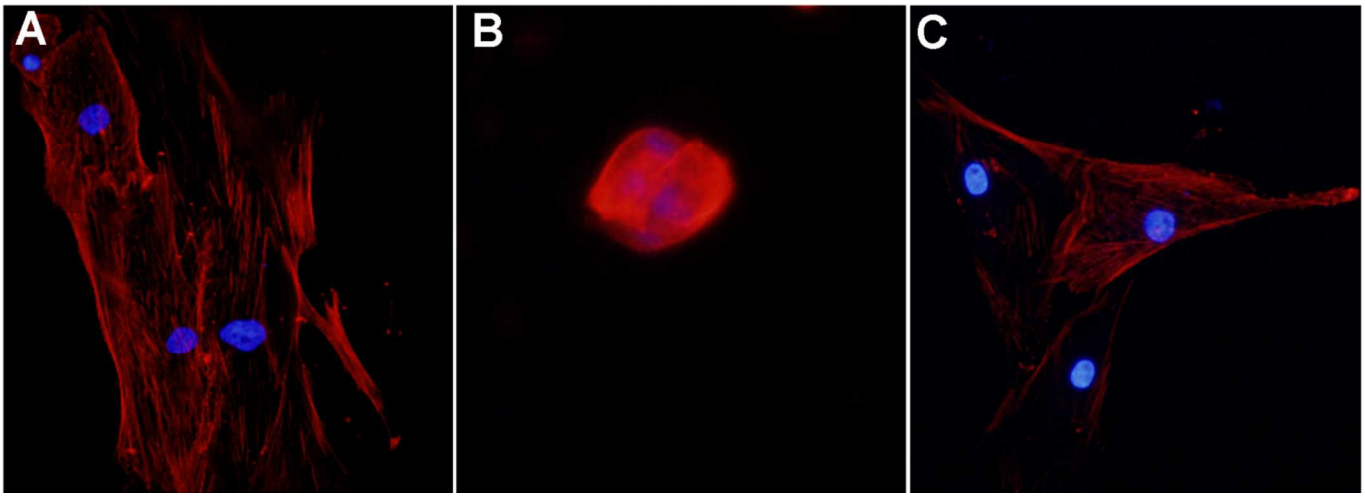

Figure 6. Fluorescence images of hMSCs cultured for 72h on the (A) TCP, (B) RGO film and (C) FN modified RGO film.

provided a smooth surface that allowed hMSCs spread freely (Figure 6A). However, hMSCs on the unmodified RGO films were rounded (Figure 6B). On the other hand, hMSCs cultured on the modified RGO films spread well and show the tendency to follow the traces of nanofibers (Figure 6C) with good cell attachment. These results indicate that the FN modified surfaces have positive effects on cell spreading, which could be attributed to the amino groups of the FN that encouraged better cell growth and retention.

The morphology of hMSCs cultured on the TCPs, the RGO and the FN modified RGO films were also studied by SEM (Figure 8). Similarly, hMSCs spread well on the TCPs (Figure 7A) while rounded on the unmodified RGO films with obvious cell-substrate boundary, i.e., loose adherence (Figure 7B). On the other hand, hMSCs cultured on the modified RGO films show the large spreading area and the cell-substrate boundary is hardly distinguishable (Figure 7C), which further indicates that hMSCs spread well and adhered tightly to the functionalized films. This may be attributed to the synergistic effects of the reactive functional groups in the FN protein and the large surface roughness and area of the graphene film.

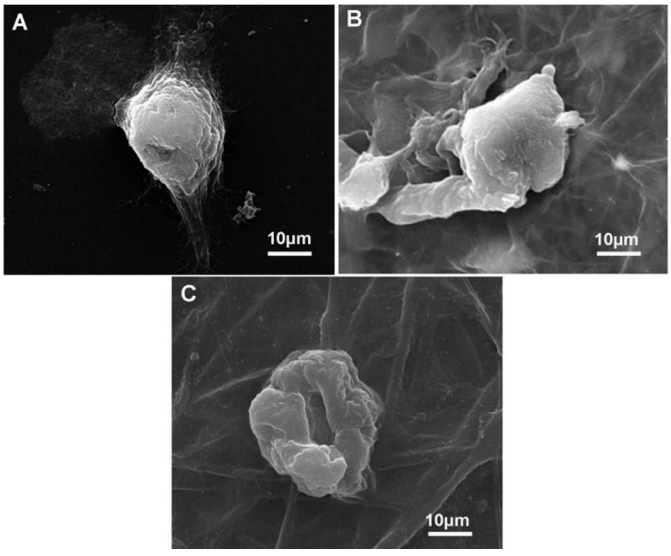

Figure 7. SEM images of hMSCs cultured for 72h on the (A) TCPs, (B) RGO film and (C) FN modified RGO film.

4. Conclusions

In this present work, we developed a novel fabrication process to successfully fabricate the free-standing RGO films with controllable nanofiber patterns by vacuum filtration of graphene oxide aqueous solution through a nanofiber membrane combining with chemical reduction. Furthermore, the obtained RGO films were coated with the FN protein to enhance cellular adhesion and proliferation. The hMSC culture results show that the obtained RGO films with protein functionalization could serve as an excellent cell culture substrate due to the synergistic effects of the reactive functional groups in the FN protein and the large surface roughness and area of the graphene films. The fabricated RGO films could also be used in many other biomedical applications, such as engineered bio-scaffold or bio-sensor.

Acknowledgements

This work was support by the National Natural Science Foundation of China (Grant No: 21404124 and 21171179). Y. Z. acknowledges the start-up research grant from the Nanyang Technological University, and the Tier-1 Academic Research Funds from the Singapore Ministry of Education (RGT 30/13 and RGC 6/13).

Notes and references

[a]School of Mechanical & Aerospace Engineering, Nanyang Technological University, 50 Nanyang Avenue, Singapore 639798, Singapore

Fax: 65-67942035; Tel: 65-67905952;
Email: ylzhang@ntu.edu.sg, zlwang2007@hotmail.com.
[b]The Key Laboratory of Rare Earth Functional Materials and Applications, Zhoukou Normal University, Zhoukou 466001, P. R. China
[c]School of Chemicall & Biomedical Engineering, Nanyang Technological University, 62 Nanyang Avenue, Singapore 637459, Singapore

Electronic Supplementary Information (ESI) available: [AFM and SEM image of the graphene oxide sheets]. See DOI: 10.1039/b000000x/

1. D. A. Dikin, S. Stankovich, E. J. Zimney, R. D. Poner, G. H. B. Dommett, G. Evmenenko, S. T. Nguyen and R. S. Ruoff, *Nature*, 2007, **448**, 457.
2. W. Jung, D. Kim, M. Lee, S. Kim, J. H. Kim and C. S. Han, *Adv. Mater.*, 2014, **36**, 6394.

3. Y. Ito, Y. Tanable. H. J. Qiu, K. Sugawara, S. Heguri, N. H. Tu, K. K. Huynh, T. Fujita, T. Takahashi, K. Tanigaki and M. W. Chen, *Angew. Chem. Int. Ed.*, 2014, **53**, 4822.
4. H. J. Yoon, T. H. Kim, Z. Zhang, E. Azizi, T. M. Pham, C. Paoletti, J. Lin, N. Ramnath, M. S. Wicha, A. F. Hayes, D. M. Simesone and S. Nagrath, *Nat. Nanotech.*, 2013, **8**, 735.
5. Y. Z. Xue, B. Wu, L. Jiang, Y. L. Guo, L. P. Huang, J. Y. Chen, J. H. Tan, D. C. Geng, B. R. Luo, W. P . Hu and Y. Q. Liu, *J. Am. Chem. Soc.*, 2012, **134**, 11060.
6. C. M. Chen, Q. H. Yang, Y. G. Yang, W. Lv, Y. F. Wen, P. X. Hou, M. Z. Wang and H. M. Chen, *Adv. Mater.*, 2009, **21**, 3007.
7. L. Jin, D. Yue, Z. W. Xu, G. B. Liang, Y. L .Zhang, J. F. Zhang, X. C. Zhang and Z. L. Wang, *RSC Adv.*, 2014, **4**,35035.
8. D. D. Kulkarni, L. Choi, S. S. Singamaneni and V.V. Tsukru, *ACS Nano,* 2010, **4**, 4667.
9. A. Cavallin, M. Pozzo, C. Africh, A. Baraldi, E. Vesselli, C. Dri, G. Comelli, R. Larciprete, P. Lacovig, S. Lizzit and D. Alfè, *ACS Nano*, 2012, **6**, 3034.
10. K. Yang, J. M. Wan, S. Zhang, B. Tian, Y. J. Zhang and Z. Liu, *Biomaterals*, 2012, **33**,2206.
11. K. Yang, Y. J. Li, X. F. Tan, R. Peng and Z. Liu, *Small*, 2013, **9**, 1492.
12. M. Zhang, L. Huang, J. Chen, C. Li and G. Q. Shi, *Adv. Mater.*, 2014, **26**, 7588.
13. B. S. Wilson, D. T. Lawson, J. M. Muller, R. S. Tyler and J. Kiefer, *Annu. Rev. Biomed. Eng.*, 2003, **5**, 207.
14. X. Navarro, T. B. Krueger, N. Lago, S. Micera, T. Stieglitz and P. Dario*, J. Peripher. Nerv. Ayst.*, 2005, **10**, 229.
15. T. Cohen-Karni, Q. Qing, Q. Li, Y. Fang and C. M. Lieber, *Nano Lett.,* 2010, **10**, 1098.
16. K. Yang, S. Zhang, G. Zhang, X. Sun, S. T. Lee and Z. Liu, *Nano Lett.*, 2010, **10**, 3318.
17. X. Sun, Z. Liu, K. Welsher, J. T. Robinson, A. Goodwin, S. Zaric and H. Dai, *Nano Res.*, 2008, **1**, 203.
18. M. Kalbacova, A. Broz, J. Kong and M. Kalbac, *Carbon*, 2010, **48**, 4323.
19. N. Li, X. M. Zhang, Q. Song, R. G. Su, Q. Zhang, T. Kong, L. W. Liu, G. Jin, M. L. Tang and G. S. Cheng, *Biomaterials*, 2011, **32**, 9374.
20. S. Y. Park, J. Park, S. H. Sim, M. G. Sung, K. S. Kim, B. H. Hong and S. Hong, *Adv. Mater.*, 2011, **23**, H263.
21. T. R. Nayak, H. Andersen, V. S. Makam, C. Khaw, S. Bae, X. Xu, P. L. Ee, J. H. Ahn, B. H. Hong, G. Pastorn and B. Zyilmaz, *ACS Nano*, 2011, **5**, 4670.
22. C. N. Yeh, K. Raidongia, J. J. Shao, Q. H. Yan and J. X. Huang, *Nat. Chem.*, 2015, DOI:10.1038/nchem. 2145.
23. A. M. Ross, Z. Jiang, M. Bastmeyer and J. Lahann, *Small*, **2012**, **8**, 336.
24. B. D. Boyan, T. W. Hummert, D. D. Dean and Z. Schwartz, *Biomaterials*, 1996, **17**, 137.
25. A. E. Nel, L. Mädler, D. Velegol, T. Xia, E. M. V. Hoek, P. Somasundaran, F. Klaessig, V. Castranova and M. Thompson, *Nat. Mater.*, 2009, **8**, 543.
26. L. Jin, T. Wang, M. L. Zhu, M. K. Leach, Y. I. Naim, J. M. Core, Z. Q. Feng and Q. Jiang, *J. Biomed. Nanotech.*, 2012, **8**, 1.
27. W. S. Hummers and R. E. Offeman, *J. Am. Chem. Soc.*, 1958, **80,** 1339.
28. N. I. Kovtyukhova, P. J. Ollivier, B. R. Martin, T. E. Mallouk, S. A. Chizhik, E. V. Buzaneva and A. D. Gorchinskiy*, Chem. Mater.*, 1999, **11,** 771.
29. L. Jin, T. Wang, Z. Q. Feng, M. K. Leach, J. H. Wu, S. J. Mo and Q. Jiang, *J. Mater. Chem. B*, 2013, **1**, 1818.
30. V. Wagner, A. Dullaart, A. K. Bock and A. Zweck, *Nat. Biotechnol.*, 2006, **24**, 1211.
31. B. Wójciak-Stothard, Z. Madeja, W. Korohoda, A. Curtis and C. Wilkinson, *Cell Biol. Int.*, 1995, **19**, 485.
32. A. C. Ferrari, J. C. Meyer, V. Scardaci, C. Casiraghi, M. Lazzeri, F. Mauri, S. Piscanec, D. Jiang, K. S. Novoselov, S. Roth and A. K. Geim, *Phys. Rev. Lett.*, 2006, **97**, 187401.
33. K. S. Kim, Y. Zhao, H. Jang, S. Y. Lee, J. M. Kim, J. H. Ahn, P. Kim, J. Y. Choi and B. H. Hong, *Nature*, 2009, **457**, 706.
34. S. H. Ku and C. B. Park, *Biomaterials*, 2013, **34**, 2017.
35. I. Y. Jeon, Y. R. Shin, G. J. Sohn, H. J. Choi, S. Y. Bae, J. Mahmood, S. M. Jung, J. M. Seo, M. J. Kim, D. W. Chang, L. Dai and J. B. Baek, *Proc. Natl. Acad. Sci. USA.*, 2012, **109**, 5588.
36. Y. Q. Li, T. Yu, T. Y. Yang, L. X. Zheng and K. Liao, *Adv. Mater.*, 2012, **24**, 3426.
37. W. C. Lee, C. H. Lim, H. Shi, L. A. Tang, Y. Wang, C. T. Lim and K. P. Lon, *ACS Nano*, 2011, **5**, 7334.
38. L. Zhuang, J. Xia, Q. Zhao and L. Liu, *Small*, 2010, **6**, 537.
39. H. Chen, M. B. Müller, K. J. Gilmore, G. G. Wallace and D. Li, *Adv. Mater.*, 2008, **20**, 3557.
40. Y. Wang, W. C. Lee, K. K. Manga, P. K. Ang, J. Lu, Y. P. Liu, C. T. Lim and K. P. Loh, *Adv. Mater.*, 2012, **24**, 4285.
41. W. Hu, C. Peng, M. Lv, X. Li, Y. Zhang, N. Chen, C. Fan and Q. Huang, *ACS Nano*, 2011, 5, 3693.
42. G. Maiorano, S. Sabella, B. Sorce, V. Brunetti, M. A. Malvindi, R. Cingolani and P. P. Pompa, *ACS Nano*, 2010, **4**, 7481.
43. S. Shah, P. T. Yin, T. M. Uehara, Y. T. D. Chueng, L. Yang and K. B. Lee, *Adv. Mater.*, 2014, **26**, 3673.
44. P. Xue, J. N. Bao, Y. J. Chuah, N. V. Menon, Y. L. Zhang and Y. J. Kang, *Langmuir*, 2014, **30**, 3110.
45. A. I. Caplan, *J. Cell Physiol.*, 2007, **213**, 341.
46. S. Kuddannaya, Y. J. Chuah, M. H. A. Lee, N. V. Menon, Y. J. Kang and Y. L. Zhang, *ACS Appl. Mater. Interface*, 2013, **5**, 9777.

Graphical Abstract

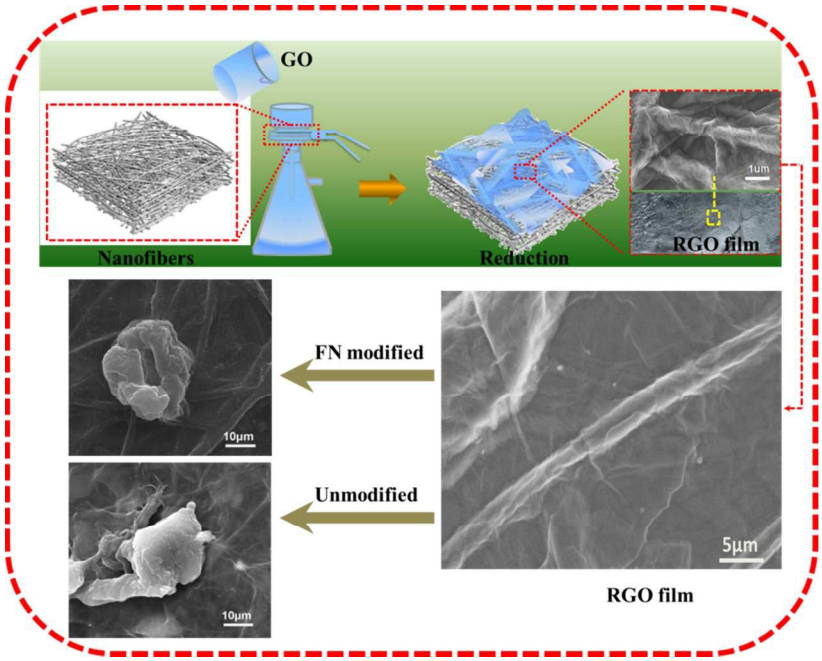

Fabrication of free-standing reduced graphene oxide (RGO) films by vacuum filtration of graphene oxide aqueous solution through a nanofiber membrane combining with chemical reduction. The obtained RGO films after fibronectin modification could exhibit excellent biocompatibility due to the synergistic effects of the RGO films including both the surface morphology and the fibronectin modification. The novel fabrication method greatly enhances the fabrication capability and the potential applications of graphene films for cell culture, tissue engineering as well as other engineering and biomedical applications.